Original Article

Hypoxia Promotes Pancreatic Cancer Malignancy via HIF-1α-induced Doublecortin-like Kinase 1 Upregulation

Rui Yan[1,&], Yunting Bai[1,&], Patiguli Yisilamu[1], Ziwei Liang[1], Guangyu An[1], Hua Fan[2], and Yang Ge[1,#]

1. Department of Oncology, Beijing Chao-Yang Hospital, Capital Medical University, Beijing 100020, China; 2. Department of Hepatobiliary Surgery, Beijing Chao-Yang Hospital, Capital Medical University, Beijing 100020, China

Abstract

Objective Pancreatic ductal adenocarcinoma (PDAC) is characterized by numerous severely hypoxic areas that drives tumor progression. Hypoxia-inducible factor-1 (HIF-1) mediates hypoxic responses mainly through HIF-1α upregulation. However, how HIF-1α influences PDAC aggressiveness remains unclear. Doublecortin-like kinase 1 (DCLK1) is overexpressed in PDAC and facilitates tumor development. This study investigated whether hypoxia regulates DCLK1 to enhance PDAC malignancy.

Methods Bioinformatics analyses of Gene Expression Omnibus (GEO) and The Cancer Genome Atlas (TCGA) datasets were used to assess the prognostic values of HIF-1α and hypoxia score, and the correlation between HIF-1α and DCLK1 expression. mRNA and protein levels of HIF-1α, DCLK1, and epithelial-mesenchymal transition (EMT) markers were detected by reverse transcription polymerase chain reaction and Western blot. Transwell assays detected cell migration and invasion after the inhibition of either HIF-1α or DCLK1. Immunofluorescence staining was performed to analyze the association among HIF-1α, DCLK1, and EMT markers in PDAC tissues.

Results Our study demonstrated significant overexpression of HIF-1α and DCLK1 in pancreatic cancer cells under hypoxic conditions. Hypoxia-driven HIF-1α upregulates DCLK1, fostering EMT and enhancing PDAC malignancy. DCLK1 inhibition in PDAC mitigates hypoxia-induced proliferation, invasiveness, and EMT progression.

Conclusion HIF-1α boosts DCLK1 in hypoxia, enhancing pancreatic cancer malignancy via EMT. Overall, targeting DCLK1 in the hypoxic tumor microenvironment of PDAC could be a promising therapeutic strategy.

Key words: Pancreatic ductal adenocarcinoma; Hypoxia; HIF-1α; DCLK1; EMT

Biomed Environ Sci, 2026; 39(x): 1-15 *doi: 10.3967/bes2026.107* *ISSN: 0895-3988*

www.besjournal.com (full text) *CN: 11-2816/Q*

INTRODUCTION

Pancreatic ductal adenocarcinoma (PDAC) is an exceptionally fatal malignancy and is the 6th leading cause of cancer-related deaths in China[1,2]. Epidemiological data have revealed a rising disease burden of pancreatic cancer in China, which is closely linked to metabolic abnormalities such as elevated fasting plasma glucose[3].PDAC is typically distinguished by numerous extensive hypoxic areas, with median tissue partial oxygen pressure (pO_2) ranging from 0

#Correspondence should be addressed to Yang Ge, M.D., E-mail: interna-1@163.com; Hua Fan, M.D., E-mail: fanhua@medmail.com.cn

Biographical notes of the first authors: Rui Yan, PhD, majoring in molecular biology of gastrointestinal and lung tumors, E-mail: yrui2019@126.com; Yunting Bai, Master candidate, majoring in molecular biology of gastrointestinal tumors, E-mail: b19800361830@163.com

to 5.3 mmHg (0%–0.7%), compared with the adjacent normal pancreas, which has a pO_2 ranging from 24.3–92.7 mmHg (3.2%–12.3%)[4]. Reportedly, Hypoxia actively contributes to tumor cell survival, progression and invasion, and closely correlate with dismal patient prognosis[4-7]. However, the mechanisms by which hypoxia leads to poorer prognoses in PDAC are still not fully understood.

Three members of the hypoxia-inducible factor (HIF) family have been identified, each comprising a heterodimeric structure with an O_2-sensitive α subunit (HIF-1α, HIF-2α, and HIF-3α) and an O_2-insensitive β subunit (HIF-1β)[8]. Among them, the transcription factor, HIF-1, a heterodimer complex comprising the HIF-1α and HIF-1β subunits, primarily mediates homeostatic response to hypoxia[9]. Previous studies have primarily focused on changes in HIF-1α protein levels within cells, and numerous studies have elucidated that under normoxia, prolyl hydroxylase (PHD) hydroxylates HIF-1α, enabling its recognition by the Von Hippel Lindau (VHL) E3 ligase, thereby triggering proteasomal degradation. Factor Inhibiting HIF (FIH) also hydroxylates HIF-1α, inhibiting its transcriptional activity. Under hypoxia, reduced PHD and FIH activity stabilize HIF-1α, allowing it to translocate to the nucleus and dimerize with HIF-1β. The HIF heterodimer binds to hypoxia-responsive elements (HREs) to regulate the transcription of the target gene[10].

Recent studies have shown that hypoxia also increases HIF-1α transcription. The promoter region of the *HIF-1α* gene contains HREs that establish an HIF-dependent autoregulatory feedback loop, and hypoxia-induced activation of nuclear factor kappa-B (NF-κB) and Egr1 additionally promotes HIF-1α mRNA expression[11]. Thus, upregulating HIF-1α under hypoxia is highly complex, with functions spanning gene and protein levels. Moreover, HIF-1α is widely recognized as significant in tumor invasion, metastasis, and therapeutic resistance[12,13]. However, the underlying mechanism by which it affects the malignant behavior of pancreatic cancer remains elusive.

Doublecortin-like kinase 1 (DCLK1), initially identified as a brain-specific protein, aids in microtubule assembly and neuronal migration[14]. DCLK1 is overexpressed in various cancers, including colorectal cancer, hepatocellular carcinoma, renal clear-cell carcinoma, and PDAC[15-18]. Furthermore, a report showed that in preinvasive pancreatic cancer, DCLK1 was used to identify a morphologically distinct and functionally unique population of cancer-initiating cells with stem cell properties[19]. Furthermore, DCLK1-positive epithelial cells have been identified as progenitors of pancreatic injury and tumor-initiating cells in PDAC[20]. However, the specific regulators underlying DCLK1 overexpression in pancreatic cancer remain unclear, and the potential correlation between DCLK1 expression and hypoxia has not been elucidated.

In this study, we found that DCLK1 expression was elevated in PDAC cell lines under hypoxia-induced HIF-1α activation. Subsequently, we observed that upregulating HIF-1α enhanced DCLK1 expression and promoted the epithelial-mesenchymal transition (EMT) program in PDAC cells. Conversely, suppressing DCLK1 expression hindered hypoxia-induced tumor proliferation and invasion. This study revealed that DCLK1 is a crucial protumor factor in the hypoxic microenvironment of PDAC, and that blocking DCLK1 has the potential to target hypoxia and improve the prognosis of patients with PDAC.

MATERIALS AND METHODS

Cell Culture and Drug Treatment

The human PDAC cell lines AsPC-1 and PANC-1, and human embryonic kidney 293T cell lines were purchased from the Academy of Medical Sciences (Beijing, China). 293T cell lines were cultured in DMEM (Biological Industries, Israel, Cat No. 01-052-1ACS). The PANC-1 cell line was cultured in DMEM, whereas the AsPC-1 cell line was cultured in RPMI 1640 under normal or hypoxic conditions. Normal conditions refer to cells maintained at a stable temperature (37 °C), a stable CO_2 level (5%), a constant pH (7.2–7.4), and a high relative humidity (95%). Hypoxic conditions involved placing both PDAC cell lines in a hypoxia chamber, which was flushed with 100 L of a gaseous mixture containing 1% O_2 and 5% CO_2 (balanced with N2), then incubating at 37 °C for 24 h. All culture media contained 10% fetal bovine serum (FBS) (ExCell Bio, China, Cat No. FSS500) and 1% penicillin-streptomycin compound (Beyotime, China, Cat No.C0222).

Construction of HIF-1α Overexpressing Cell Lines

HIF-1α isoform sequences were cloned into the pCDH-MSCV-MCS-EF1-puro vector to construct overexpressing cell lines. The constructed plasmids and packaging plasmids, including pMD_2G and $psPAX_2$, were co-transfected into 293T packaging cells using Lipofectamine 3000

(Invitrogen, USA) for lentiviral amplification, and the lentiviruses were obtained 48 h and 72 h post-transfection. Next, the harvested viruses were filtered through 0.45 μm filters and co-cultivated with PDAC cell lines (AsPC-1 and PANC-1). After 3 days of co-cultivation, cells stably overexpressing HIF-1α were selected with 2 μmol/L puromycin to construct stable cell lines.

Establishment of HIF-1α and DCLK1 Knockdown Cell Lines

Short hairpin RNA (shRNA) plasmids targeting HIF-1α (target sequence: 5′-TATGCACTTTGTCG CTATTAA-3′) and DCLK1 (target sequence: 5′-CAGGTATCTTTGTAGCGGTTT-3′) were used in this study. Following lentiviral packaging performed with the protocol described above, AsPC-1 and PANC-1 cells were transduced with the packaged lentiviral particles. Stable HIF-1α and DCLK1 knockdown cell lines were obtained after selection with puromycin.

Transwell Migration and Invasion Assay

The assay includes two components: a migration assay (uncoated inserts to assess directional motility) and an invasion assay (Matrigel-coated inserts to evaluate barrier penetration). Higher transmembrane cell numbers indicate stronger migratory/invasive malignant behaviors.

For the migration assay, 5×10^4 cells suspended in FBS-free medium were inoculated into the upper chamber of the Transwell insert, and complete culture medium was added to the lower chamber as a chemoattractant. The invasion assay was carried out using the same protocol as the migration assay, except that the upper chamber insert was pre-coated with Matrigel prior to cell seeding. After incubation at 37 °C for 24 h, the cells at the bottom were fixed with 4% paraformaldehyde for 15 min, then stained with 0.1% crystal violet. Cell counting was performed using an inverted light microscope. For each well, 3 to 5 random fields of view were selected for analysis. The number of migrated cells was quantified using ImageJ software (NIH, USA). Parameter settings: Image Type: 8-bit; Adjust Threshold: 0/128; Process: Binary→Watershed; Analyze Particles: Size threshold = 0.01. Data are presented as the mean number of cells per field of view ± SEM from three independent experiments.

RNA Extraction and Quantitative RT-PCR

Total RNA was extracted from the cells using the Trizol reagent (Yeasen, China, Cat No.10606ES60) according to the manufacturer's instructions. Utilizing 1 μg of total RNA, cDNA was synthesized in a 20 μL reverse transcription reaction using PrimeScript (Yeasen, China, Cat No. 11137ES60). To assess the expression levels of HIF-1α and DCLK1 mRNA, real-time PCR analysis was conducted on the 7500 Sequence Detection System (Applied Biosystems, China). This was achieved using the SYBR Green Premix (Yeasen, China, Cat No. 11203ES) according to the manufacturer's guidelines. All experiments were conducted in triplicate to ensure consistency and reliability. The expression levels of mRNA were confirmed by the $2^{-\Delta\Delta CT}$ method after normalization to β-actin. Supplementary Table S1 presents the primer sequences.

ChIP-qPCR

ChIP-qPCR was performed using the BeyoChIP™ ChIP Assay Kit (P2080S, Beyotime, China) with Protein A/G magnetic beads according to the manufacturer's instructions. Cellular proteins and genomic DNA were cross-linked with 1% formaldehyde, and chromatin was sonicated into 200–1,000 bp fragments. Input control, HIF-1α immunoprecipitation group and IgG negative control group were set up. After immunoprecipitation, sequential washing, elution and decrosslinking, the precipitated DNA was purified for qPCR detection. The core sequence of the conserved HRE in the DCLK1 regulatory region was 5'-ACGTG-3'. The primers targeting the HRE-containing region of the DCLK1 promoter were as follows: forward primer, 5'-TCTCTCTCTCACCGGACCAAGCA-3'; reverse primer, 5'-CTTTGCGGAGAGGAAATGGGCA-3'. All experiments were performed in triplicate. The ΔCt value for each immunoprecipitated sample was calculated as ΔCt = ChIP Ct − Input Ct. The relative enrichment of the target DNA fragment was then determined using the formula: Relative enrichment = $2^{-\Delta\Delta CT}$.

Protein Extraction and Western Blot

Proteins were extracted using RIPA lysis buffer (Beijing Solarbio Science & Technology, China, Cat No. R00010). Thereafter, the protein concentration was quantified using a bicinchoninic acid (BCA) detection kit (Thermo Fischer Scientific, Inc.). Proteins (40 μg/lane) were denatured, loaded onto a 10% gel, and analyzed *via* SDS-PAGE. Subsequently, the proteins were transferred to PVDF membranes using a semi-dry method at 200 mA for 1.5 h. (EMD Millipore). After overnight incubation with primary antibodies at 4 ˚C, the membranes were incubated for 1 hour at room temperature (RT) with either a

horseradish peroxidase-conjugated secondary goat anti-rabbit or anti-mouse-polyclonal immunoglobulin G antibody. The signals were visualized using an enhanced chemiluminescence kit (Applygen Technologies, Inc.). Supplementary Table S2 presents detailed information regarding all antibodies used in this study. Western blot band intensities were quantified using ImageJ software. The intensity of each target protein band was normalized to the β-actin.

Immunofluorescence

Special glass cover slides (Absin, China, Cat No. abs7027) for cell immunofluorescence were placed into 24-well plates (Nest, USA, Cat. No. 801006) in advance. AsPC-1 and PANC-1 pancreatic cancer cells were seeded at a density of 3×10^4 cells per well on glass coverslips. After culturing for 24 h to reach 70% confluence, the cells were fixed with 4% formaldehyde in PBS for 15 min at room temperature. Then, the cells were blocked with 2% bovine serum albumin in PBS (PBA) for 1 h and incubated with the primary antibody against E-cadherin (1:150, Proteintech, USA, Cat No. 60335-1-Ig), Vimentin (1:100, Proteintech, USA, Cat No. 10366-1-AP), DCLK1 (1:500, Abcam, USA, Cat No. ab137526) and HIF-1α (1:1,000, Proteintech, USA, Cat No. 10366-1-AP) in 2% PBA overnight at 4 °C. The cells were washed and incubated with a secondary antibody conjugated to (fluoscein isothiocyanate (FITC) (Proteintech, USA, Cat No. SA00003-2)), and TRITC (Proteintech, USA, Cat No. SA00007-2), and incubated with DAPI (ZSBG-bio, China, Cat No. ZLI-9557). Images were captured using a fluorescence microscope and analyzed with ImageJ software (National Institutes of Health, USA). Regions of interest (ROI) were manually annotated on the multiplex immunofluorescence images using QuPath software. The expression level of target protein within each ROI was quantified as the mean fluorescence intensity (MFI), which was calculated as the mean gray value of all pixels within the annotated region. Background autofluorescence was subtracted based on negative control regions to ensure accurate signal quantification.

Immunohistochemistry

Pancreatic cancer TMA was purchased from Shanghai Outdo Biotech Co., Ltd. (Shanghai, China; batch No. SHYJS-CP-240106). This study was approved by the Ethics Committee of Shanghai Outdo Biotech Co., Ltd. and complied with the ethical standards for human tissue research. Tumor Grade was determined according to the World Health Organization classification system, and detailed clinicopathological information of the patients is provided in Supplementary Table S3. Tumor tissues were fixed in 4% paraformaldehyde (Solarbio, Beijing, China), embedded in paraffin, and sectioned at 6 μm for IHC analysis. Briefly, tissue sections were deparaffinized in xylene for 30 min and hydrated in a descending alcohol series (100%, 95%, and 80% alcohol) for 5 min each. After antigen retrieval with EDTA (ZSGB-BIO, China) and blocking with goat serum for 1 hour at room temperature, the sections were incubated with the corresponding antibody at 4 °C overnight, followed by incubation with enhanced enzyme-labeled goat anti-mouse/rabbit IgG polymer (ZSGB-BIO, China). The IHC signal was detected using 3,3′-diaminobenzidine (DAB, ZSGB-BIO, China). The antibodies used above were: anti-HIF-1α (1:1,000, ab183685, Abcam), anti-DCLK1 (1:500, ab31704, Abcam), anti-E-cadherin (1:500, 3195T, Cell Signaling Technology), anti-Vimentin (1:500, AF-585-NA, R&D).

Subcutaneous Graft Tumor Model in Nude Mice

Female BALB/c nude mice aged 5–6 weeks were obtained from Charles River Laboratory (Beijing, China). Mice were randomly divided into three groups (n = 5 per group) to establish a subcutaneous tumor model. Each mouse was subcutaneously injected with 100 μL of either PANC-1 Vector or PANC-1 HIF-1α-OE cell suspension (containing 2×10^6 cells). Tumor sizes were measured every 5 d and calculated using the following formula: volume = (length × width ^{2})/2. In the PANC-1-HIF-1α-OE cohort, a subset was administered DCLK1-IN-1 (10 mg/kg/day, i.p.), whereas other groups received DMSO as controls.

Lung Metastasis Model in NOD-SCID Mice

Female NOD-SCID mice aged 5 weeks were selected and randomly divided into 3 groups with 5–6 mice in each group. Mice in the control group were injected with 1×10^7 AsPC-1 Vector Control cells, while the remaining two groups were injected with 1×10^7 AsPC-1 HIF-1α-OE cells via tail vein. One week after tail vein injection, one group of mice injected with AsPC-1-HIF-1α-OE cells received intraperitoneal injection of the DCLK1 inhibitor DCLK1-IN-1 (10 mg/kg/day), and the other two groups received intraperitoneal injection of solvent as control. After 30 days, the mice were dissected to observe lung tumor metastasis in each group. All animal experiments were approved by the

Institutional Animal Care and Use Committee of the Capital Medical University. The ethical approval number is:25-2157.

RNA-seq Data from Public Databases

The level of mRNA expression data of HIF-1α (RNA-seq) of patients with PDAC in the TCGA database (Cohort: TCGA-PDAC) was collected from UCSC Xena (http://xena.ucsc.edu/) to investigate the correlation between the expressions of HIF-1α and DCLK1. The "ggcorrplot" R package was used to plot the correlation heat map, and the cor () function was used to calculate the Spearman correlation coefficient. Additionally, RNA-seq and survival data for 139 patients were curated from the GEO (GSE183795) cohort, and 134 of these were selected as the external validation cohort for subsequent analyses.

Calculation of Hypoxia Score

To quantify intratumoral hypoxia burden, single-sample gene set enrichment analysis (ssGSEA) was performed against the HALLMARK_HYPOXIA gene signature downloaded from MSigDB database, and the resulting enrichment score was defined as hypoxia score for each individual patient. For survival stratification, all patients in discovery cohort were separated into high-hypoxia and low-hypoxia subgroups using the median value of hypoxia score as predefined cutoff. Kaplan-Meier survival analysis with log-rank test was utilized to compare overall survival difference between two hypoxia subgroups in both cohorts, and an independent external validation cohort (GSE183795) was adopted to verify the prognostic findings.

Statistical Analysis

Data analysis was performed using the GraphPad Prism software (version 6.0; GraphPad Software, RRID: SCR_002798). For parametric analyses, the Student's *t*-test was used to assess statistical differences. Multiple group comparisons were analyzed using one-way *ANOVA*, with intergroup differences further delineated using Tukey's post-hoc test. For survival analysis, Kaplan-Meier survival curves were generated, and differences between groups were compared using the log-rank test. Categorical data were analyzed using Fisher's exact test. Quantitative data are presented as the mean ± standard deviation. Statistical significance was set at $P < 0.05$. Asterisks indicate different levels of significance: *$P < 0.05$, **$P < 0.01$, ***$P < 0.001$, and ****$P < 0.0001$.

RESULTS

Hypoxia Score and HIF-1α Expression are Associated with Poor Prognosis in Pancreatic Cancer

First, the intratumoral hypoxia status of 178 patients with pancreatic cancer was quantified using single-sample Gene Set Enrichment Analysis (ssGSEA) based on a well-validated hypoxia-related gene set (HALLMARK_HYPOXIA from MSigDB). Thereafter, patients were stratified into high- and low-hypoxia score groups using the median hypoxia score as the cutoff. Patients in the high-hypoxia score group exhibited significantly poorer overall survival than those in the low-hypoxia score group (Figure 1A, left panel). Furthermore, the above result was also validated in an independent external validation GEO cohort (GSE183795) (Figure 1A, right panel).

A central mediator of the cellular response to hypoxia is the transcription factor HIF-1α, which plays an important part in hypoxia score[8,21]. Analysis of the TCGA-PDAC dataset revealed that HIF-1α expression was remarkably upregulated in tumor tissues compared with adjacent normal tissues (Figure 1B). In the GSE183795 cohort, patients with high HIF-1α mRNA levels were significantly associated with poor survival (Figure 1C). Furthermore, to investigate the clinical significance of HIF-1α in PDAC, we performed IHC staining of HIF-1α in a cohort of 15 PDAC tissues. The IHC images showed that the staining intensity of HIF-1α gradually increased with increasing pathological grade (Figure 1D). Quantification analysis revealed that the HIF-1α H-score in Grade III tumors was significantly higher than that in Grade I and Grade II tumors (Figure 1E). Collectively, our findings suggest that HIF-1α plays a pivotal role in PDAC.

Hypoxia Promotes the Migration, Invasion, and EMT Process in PDAC Cells

To investigate whether hypoxia contributes to tumor progression, a series of *in vitro* assays was conducted to assess the effects of hypoxic conditions on the functional properties of pancreatic tumor cells. Pancreatic tumor cells were cultured under both normoxic and hypoxic conditions for 24 h, and the migratory and invasive capacities of two PDAC cell lines, PANC-1 and AsPC-1, were evaluated using a Transwell migration assay. Hypoxia enhanced the invasive and migratory activities compared with those of pancreatic tumor cells cultured under normal conditions (Figure 2A). Alterations in cancer

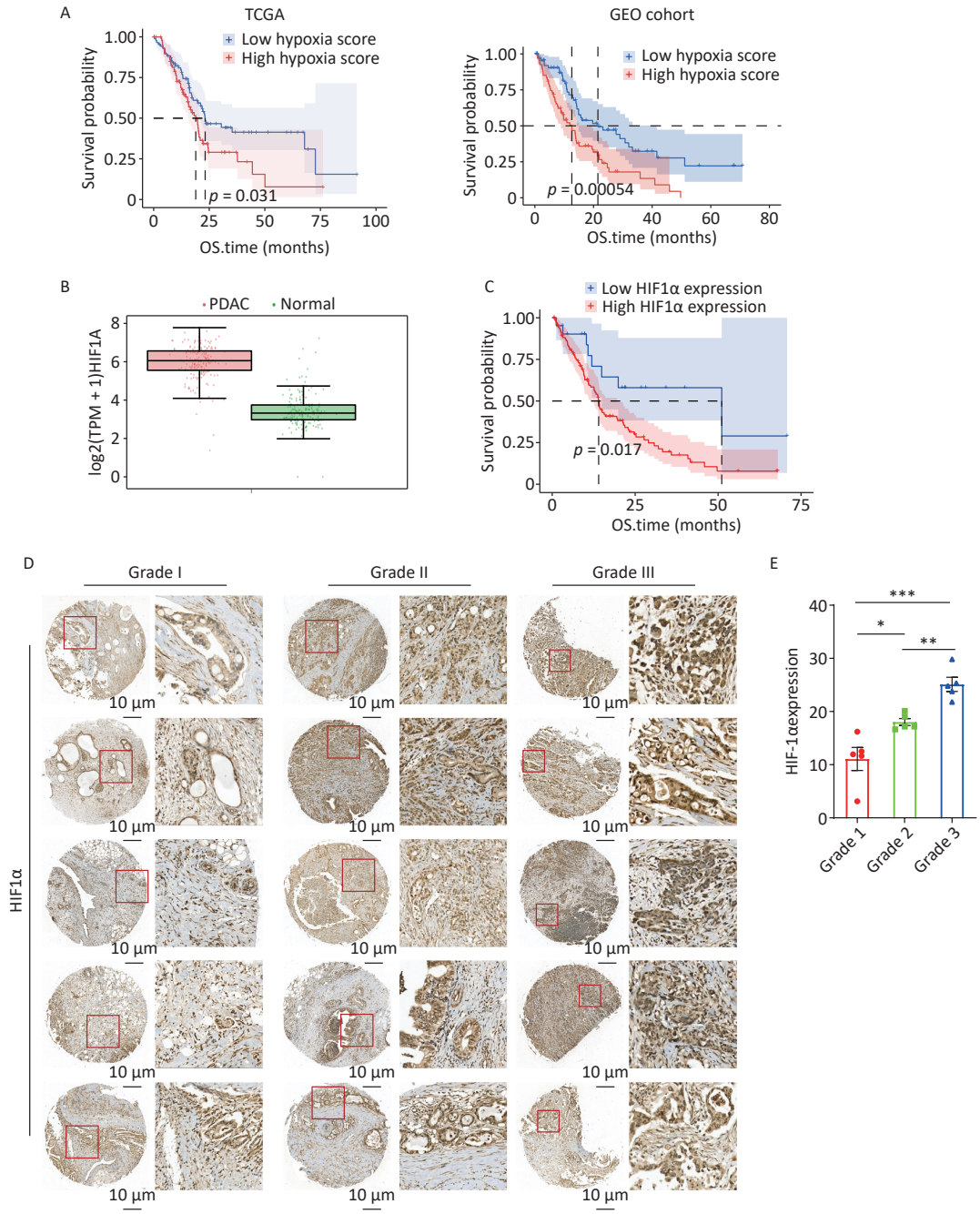

Figure 1. Hypoxia score and HIF-1α expression are associated with poor prognosis in pancreatic cancer. A. The overall survival (OS) of the high hypoxia score and low hypoxia score groups in the The Cancer Genome Atlas (TCGA)-pancreatic ductal adenocarcinoma (PDAC) cohort (Log-rank test, *P* = 0.031, left panel). Validation of the prognostic impact of hypoxia score on the OS in the independent GSE183795 cohort (Log-rank test, *P* = 0.00054, right panel). B. Hypoxia-inducible factor-1α (HIF-1α) mRNA expression in PDAC versus peritumoral normal tissue from TCGA. C. The OS of the high-HIF-1α expression and low-HIF-1α expression groups in the GSE183795 cohort (Log-rank test, *P*=0.017). D. The images of immunohistochemistry (IHC) staining for HIF-1α in PDAC tissues with diverse pathological grades (Grade I, II, III). Scale bars indicate 10 μm. E. Quantification of HIF-1α IHC staining intensity in PDAC tissues (*n* = 15). Statistical significance was determined by one-way *ANOVA* followed by Tukey's post-hoc test. For all bar-plots, mean ± SEM. **P* < 0.05, ***P* < 0.01, ****P* < 0.001.

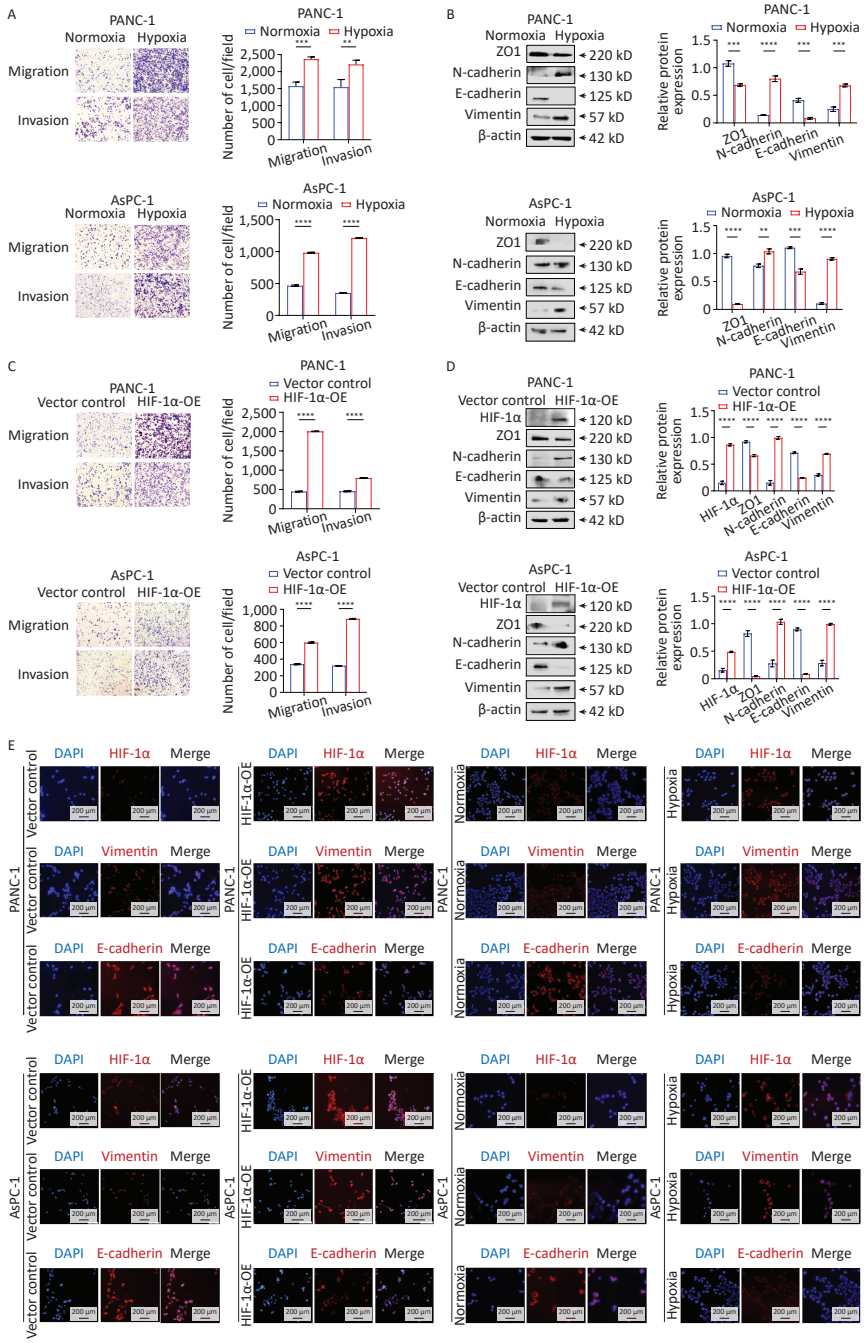

Figure 2. Hypoxia and HIF-1α overexpression promote the migration, invasion, and EMT process of PDAC cells. A. Transwell assays to evaluate the effect of hypoxia and normoxia on the migration and invasion properties of two pancreatic ductal adenocarcinoma (PDAC) cell lines, PANC-1 and AsPC-1. B. Western blot was utilized to evaluate the expression levels of epithelial-mesenchymal transition (EMT) markers in PDAC cells under hypoxia or normoxia for 24 h. C. Transwell assays to evaluate the effect of hypoxia-inducible factor-1α (HIF-1α) overexpression (HIF-1α-OE) on the migration and invasion properties of PDAC cells. D. Western blot detection of EMT markers upon HIF-1α overexpression. E. Immunofluorescence staining was utilized to observe HIF-1α, E-cadherin, and Vimentin in two PDAC cell lines under hypoxic conditions or after HIF-1α overexpression. Statistical significance was determined using the unpaired Student's *t*-test. Comparisons of differences between groups were indicated by **P* < 0.05, ***P* < 0.01, ****P* < 0.001, *****P* < 0.0001. For all bar plots, the mean ± SEM was shown; *n* = 3.

cell migration and invasion capacities are commonly linked to EMT. Therefore, we detected expression of EMT-related markers, including the epithelial markers E-cadherin and ZO1, and the mesenchymal markers N-cadherin and Vimentin. Western blotting results showed a significant increase in the expression of N-cadherin and Vimentin, and a significant reduction in the expression of E-cadherin and ZO1 in PDAC cells under hypoxia (Figure 2B). In addition, we detected the expression of the transcription factor Slug and ZEB1, another key effector of EMT. The results showed that hypoxia upregulated the expression of ZEB1 and Slug, indicating the activation of the EMT program (Supplementary Figure S1A).

Subsequently, we explored the role of HIF-1α in EMT in pancreatic cancer. We generated two stable cell lines with HIF-1α overexpression (OE) (PANC-1 HIF-1α-OE and AsPC-1 HIF-1α-OE). Compared with parental cells, HIF-1α-overexpressing cells exhibited classic EMT features, including increased migratory and invasive capabilities in the transwell assay (Figure 2C). Consistently, HIF-1α overexpression was linked to downregulation of epithelial markers, such as ZO-1 and E-cadherin, as well as to an upregulation of mesenchymal markers, including N-cadherin and Vimentin (Figure 2D), and also upregulates the expression of EMT transcription factors Slug and ZEB1 (Supplementary Figure 1B). We further validated these findings using immunofluorescence staining (Figure 2E). Collectively, our findings suggest that HIF-1α can activate EMT in PDAC under hypoxic conditions.

HIF-1α Induces DCLK1 Expression in PDAC under Hypoxia

Recent studies reveal that DCLK1 is overexpressed and is important in PDAC progression[22,23]. Consequently, we aimed to explore the potential association between DCLK1 and HIF-α expression in PDAC. Using TCGA-PDAC data, we analyzed the expression of 15 HIF pathway genes and DCLK1 in 179 patients with PDAC. Heatmap analyses consistently revealed a positive correlation between DCLK1 and HIF-1α expression (Figure 3A). To assess the expression of DCLK1 and HIF-1α in response to hypoxic induction, cells were exposed to hypoxia for 24 h. Real-time PCR and Western blot demonstrated that the expression of both HIF-1α and DCLK1 substantially increased (Figures 3B, 3C). Additionally, our results revealed an increase in DCLK1 expression upon HIF-1α overexpression, as evidenced by Western blot and immunofluorescence imaging, suggesting that DCLK1 expression is regulated by HIF-1α (Figures 3D, 3E).

To further clarify whether the upregulation of DCLK1 in PDAC cells upon hypoxic induction is induced by HIF-1α, we treated the cells with HIF-1α inhibitor BAY87-2243 (10 μmol/L) under hypoxic conditions. As anticipated, BAY87-2243 treatment reduced HIF-1α expression and downregulated DCLK1 (Figure 3F, upper panel). To rule out non-specific effects of the HIF-1α inhibitor BAY87-2243, we knocked down HIF-1α in hypoxic-cultured PDAC cells, and observed that DCLK1 expression also exhibited a downward trend (Figure 3F, lower panel). To further determine whether HIF-1α directly modulates DCLK1 expression, we performed chromatin immunoprecipitation with quantitative PCR (CHIP-qPCR) assays, which confirmed that HIF-1α directly binds to the HRE motif within the regulatory region of DCLK1 (Figure 3G). Collectively, our findings demonstrate that hypoxia-induced upregulation of HIF-1α mediates DCLK1 expression in PDAC cells, and this regulatory effect is a direct transactivation of DCLK1 by HIF-1α.

HIF-1α Promotes Hypoxia-induced Malignancy in PDAC Cells via DCLK1 Upregulation

To further explore whether DCLK1 mediates hypoxia-induced malignancy in pancreatic cancer, PANC-1 and AsPC-1 cells were exposed to hypoxic conditions in the presence or absence of a DCLK1 inhibitor.

For pharmacological inhibition of DCLK1, the selective inhibitor DCLK1-IN-1 was used in cell treatment. Distinguished from conventional DCLK1 inhibitors including LRRK2-IN-1, XMD8-92, and XMD8-85, which exhibit broad-spectrum inhibitory activity and simultaneously suppress multiple off-target molecules such as ERK5, LRRK2, and BRD4, DCLK1-IN-1 is a novel engineered compound with exclusive selectivity for DCLK1 and no non-specific cross-reactivity. Whole-kinome profiling and dedicated functional assay validation have verified that DCLK1-IN-1 exerts no inhibitory effects on ERK5, BRD4, or LRRK2 at therapeutically effective concentrations.

Consistent with previous pharmacological studies of gastrointestinal malignancies, including colorectal, pancreatic, and esophageal cancers, DCLK1-IN-1 at concentrations of 2.5–10 μmol/L can efficiently and specifically suppress endogenous DCLK1 activity without detectable off-target responses[24]. Based on the validated effective concentration range and to ensure stable inhibitory efficiency as well as

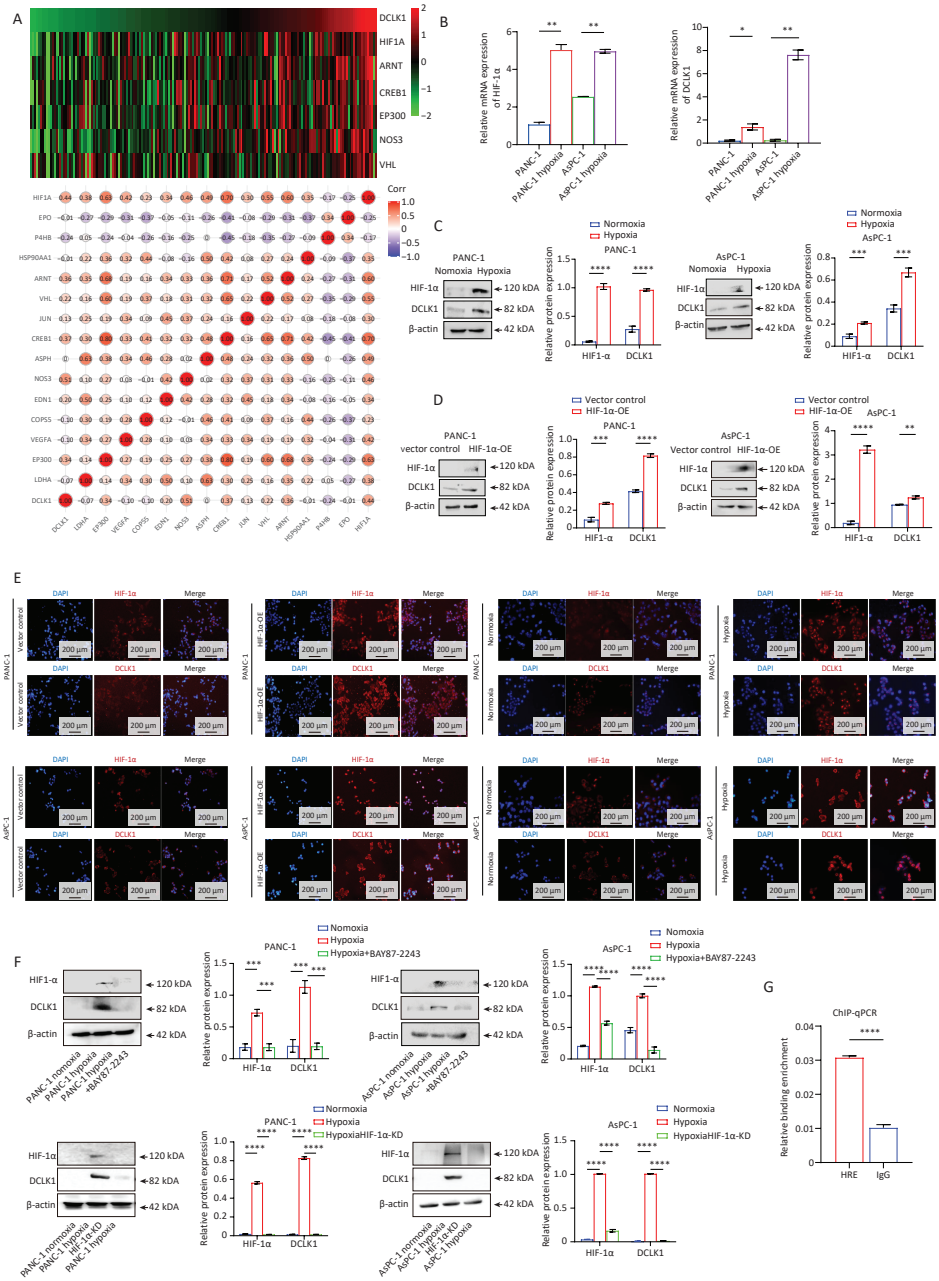

Figure 3. HIF-1α mediates hypoxia-induced DCLK1 expression in PDAC. Positive correlation between hypoxia-inducible factor-1α (HIF-1α) and doublecortin-like kinase 1 (DCLK1) expression revealed by The Cancer Genome Atlas (TCGA)-dataset analysis via Spearman correlation analysis. Upper panel, Spearman correlation visualization; lower panel, heat map visualization. B. Real-time PCR was conducted to analyze the HIF-1α and DCLK1 mRNA expression levels in pancreatic ductal adenocarcinoma (PDAC) cells under normoxia or hypoxia. C. Western blot for HIF-1α and DCLK1 protein under normoxia or hypoxia. D. Western blot assays to evaluate DCLK1 protein expression in PANC-1 and AsPC-1 cell lines after HIF-1α-OE. E. Immunofluorescence staining of HIF-1α and DCLK1 in two PDAC cells treated with hypoxia or HIF-1α-OE. F. Western blot showing DCLK1 protein alterations in hypoxic PDAC cells treated with the HIF-1α inhibitor BAY87-2243 (10 μmol/L) or knockdown of HIF-1α. G. ChIP-qPCR results indicate that HIF-1α directly regulates DCLK1. Statistical significance was determined using the Student's *t*-test. Comparisons of differences between groups were indicated by **P* < 0.05, ***P* < 0.01, ****P* < 0.001, and *****P* < 0.0001. For all bar plots, the mean ± SEM was shown; *n* = 3.

experimental reproducibility, 5 μM DCLK1-IN-1 was adopted as the optimal intervention concentration for all cellular functional experiments in the present work.

As predicted, DCLK1 inhibition significantly attenuated cell migration and invasion under hypoxia in the Transwell assay (Figure 4A). Furthermore, inhibiting DCLK1 under hypoxic conditions significantly reduced the expression of the mesenchymal marker, Vimentin; however, epithelial markers ZO-1 and E-cadherin were upregulated (Figure 4B). To exclude the off-target effect of DCLK1 inhibitors, we knocked down DCLK1 in PDAC cells cultured under hypoxic conditions, then re-evaluated the invasion and migration abilities of the cells, and compared the changes of molecular markers related to the EMT process among groups. The results still showed that DCLK1 knockdown can reduce the hypoxia-induced increase in cell invasion and migration abilities, and reverse the EMT process (Supplementary Figures S2A, 2B).

To confirm the role of DCLK1 downstream of HIF-1α in promoting malignancy, we treated HIF-1α-overexpressing PANC-1 and AsPC-1 cells with a DCLK1 inhibitor and performed functional assays. Transwell assays showed that DCLK1 inhibitors blocked HIF-1α-enhanced migration and invasion (Figure 4C). In line with this, both western blot and immunofluorescence imaging results showed that inhibiting DCLK1 reduced mesenchymal marker expression, whereas it increased epithelial marker expression in HIF-1α overexpressed cells (Figures 4D, 4E). In DCLK1 knockdown experiments, we also observed results consistent with those obtained with DCLK1 inhibitors (Supplementary Figures S2C, 2D). Overall, our results indicate that hypoxia-induced HIF-1α overexpression enhances the tumorigenic potential of pancreatic cancer cells by upregulating DCLK1, and that inhibiting DCLK1 effectively reduces hypoxia-induced cell migration and invasion.

Additionally, to further validate the aforementioned findings *in vivo*, we performed subcutaneous tumor formation using PANC-1-Vector and PANC-1-HIF-1α-OE cells. Among the PANC-1-HIF-1α-OE group, one subset received intraperitoneal injections of the DCLK1 inhibitor (DCLK1-IN-1, 10 mg/kg/day), whereas the other two groups were treated with DMSO solvent as a control. The results showed that the tumor burden in the PANC-1-HIF-1α-OE group was significantly higher than that in the PANC-1 control group. However, DCLK1-IN-1 administration inhibited subcutaneous tumor formation in the PANC-1-HIF-1α-OE group (Figure 5A-5C) without affecting the status of the mice, as evidenced by no significant changes in body weight (Figure 5D).

To further confirm that DCLK1 mediates the promotional effect of HIF-1α on distant metastasis of pancreatic cancer cells, the AsPC-1 pancreatic cancer cell line, which exhibits strong propensity for distant metastasis, was selected for subsequent *in vivo* validation, and we established a tail vein injection-induced lung metastasis mouse model. The results demonstrated that lung metastatic lesions were markedly more severe in the HIF-1α overexpression group compared with the control group and the DCLK1 inhibitor-treated group. Specifically, diffuse morphological alterations were observed in the lung tissues of mouse No. 1 and No. 2, with the entire lung parenchyma displaying a gray-white appearance in the HIF-1α overexpression group. By contrast, only one mouse developed a solitary pulmonary metastatic lesion in either the control or the DCLK1 inhibitor-treated group (Figure 5E). Collectively, these findings reveal that DCLK1 inhibition significantly reverses the metastatic potential driven by HIF-1α overexpression. These findings confirm that targeting DCLK1 can counteract the tumor-promoting effects of HIF-1α.

High HIF-1α Expression is Associated with DCLK1 Overexpression and EMT Activation in Patients with PDAC

To explore the spatial correlation of HIF-1α, DCLK1, and EMT program markers in pancreatic cancer, we performed multiplexed immunofluorescence analysis of patient-derived tumor tissue microarrays (TMA). Overall, 24 PDAC tumor samples were included in the analysis. Representative images of multiplexed immunofluorescence stained for DCLK1, HIF-1α, Vimentin, and E-cadherin from two consecutive microarrays were presented in Figure 6.

Notably, DCLK1 expression was tightly correlated to HIF-1α, with both expression levels significantly higher in cancerous than in pericancerous tissues. Additionally, decreased expression of E-cadherin and increased expression of Vimentin were observed in patients with higher DCLK1 and HIF-1α expression (Figure 6A, 6B). Subsequently, in pancreatic cancer tissues, using the mean fluorescence intensity (MFI) of HIF-1α-expression level as the cutoff value, we classified the tumors into high- and low-HIF-1α groups. We found that the high-HIF-1α group exhibited significantly elevated expression levels of DCLK1 and Vimentin compared to the low-HIF-1α

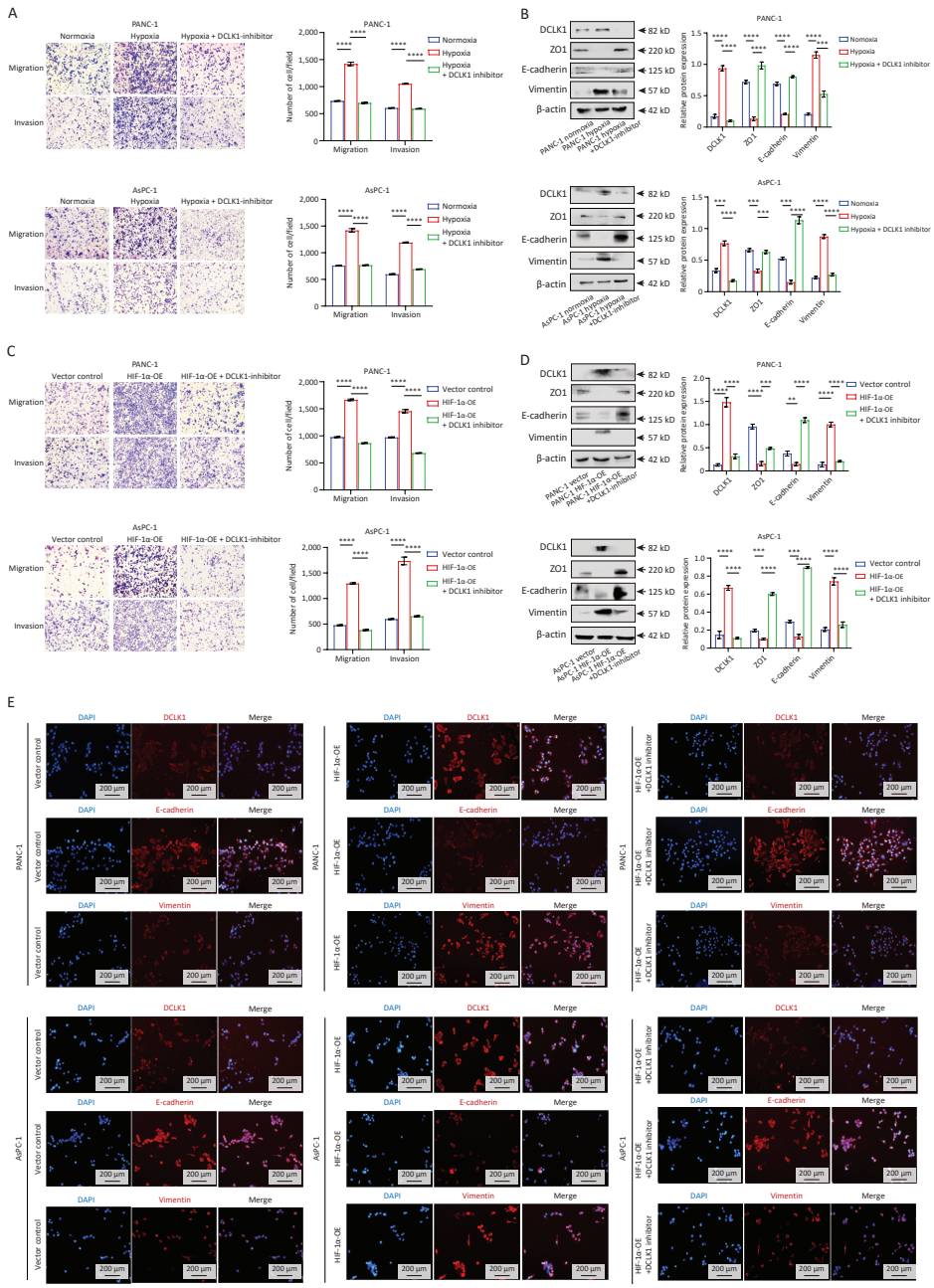

Figure 4. HIF-1α promotes hypoxia-induced malignancy in PDAC cells via DCLK1 activation. A. Transwell assays were used to investigate the effect of doublecortin-like kinase 1 (DCLK1) on hypoxia-induced cell migration and invasion. B. Western blot to evaluate the effect of the levels of epithelial-mesenchymal transition (EMT)-related proteins in treated pancreatic ductal adenocarcinoma (PDAC) cells with the DCLK1 inhibitor DCLK1-IN-1 (5 μmol/L) under hypoxia. C. Transwell assays were conducted to evaluate the effect of DCLK1 on cell migration and invasion, which were induced by hypoxia-inducible factor-1α (HIF-1α) overexpression. D. Western blot was performed to evaluate the effect of the levels of EMT-related proteins in cells treated with PANC-1 HIF-1α-OE and AsPC-1 HIF-1α-OE with the DCLK1 inhibitor. E. Immunofluorescence staining of DCLK1, E-cadherin, and Vimentin in PDAC cells treated with Vector control, HIF-1α-OE, or HIF-1α-OE+DCLK1-IN-1 (5 μmol/L). Statistical significance was determined using the unpaired Student's *t*-test. Comparisons of differences between groups are indicated by **P* < 0.05, ***P* < 0.01, *** *P*< 0.001, and *****P* < 0.0001. For all bar plots, the mean ± SEM was shown; *n* = 3.

group. Conversely, the expression levels of E-cadherin were notably lower in the high-HIF-1α group (Figure 6C). Overall, our data reveal the clinical link between HIF-1α and DCLK1 expression and their role in EMT in PDAC.

DISCUSSION

PDAC accounts for more than 90% of all pancreatic malignancies, and patients with PDAC exhibit a poor 5-year overall survival rate of less than 8%[25,26]. As a defining hallmark of the PDAC tumor microenvironment, hypoxia is strongly associated with poor clinical outcomes, and multiple studies have confirmed that hypoxia upregulates HIF-1α expression[27,28]. However, whether HIF-1α upregulation enhances malignant behavior in PDAC remains incompletely understood. In this study, we

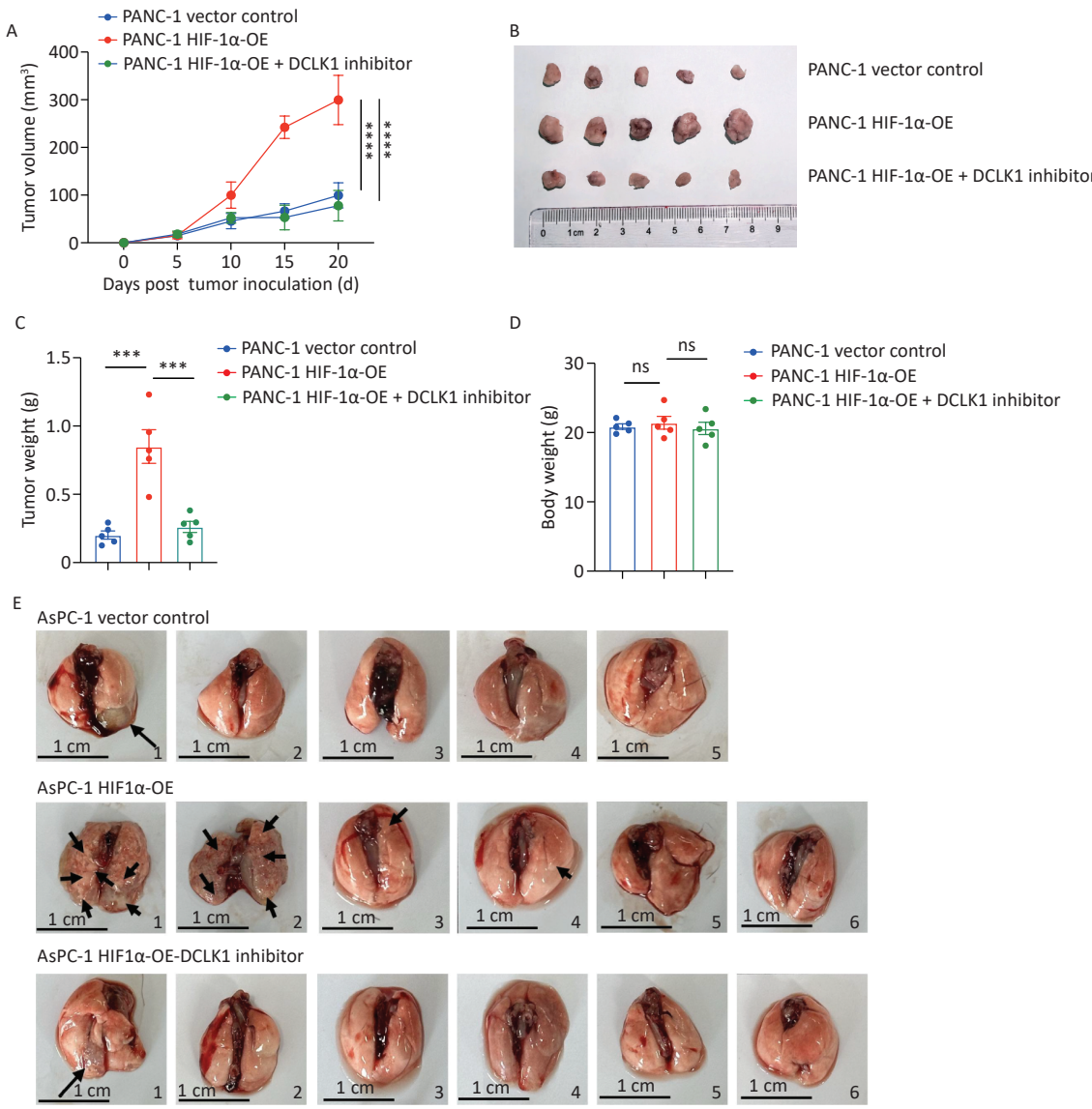

Figure 5. DCLK1 inhibition blocks HIF-1α-induced tumorigenesis *in vivo.* A. Tumor growth curves of three mouse groups: PANC-1 Vector control, PANC-1 HIF-1α-OE, and PANC-1 HIF-1α-OE + DCLK1 inhibitor. B. Representative images of tumors from each group. C. Final tumor weights in each group. D. Final body weight of the mice in each group. Statistical significance was determined using the student's *t*-test. E. Representative lung photographs show that DCLK1 inhibition reverses HIF-1α overexpression-promoted lung metastasis of pancreatic cancer. ***$P < 0.001$, ****$P < 0.0001$; comparisons: HIF-1α-OE vs. Vector and HIF-1α-OE vs. HIF-1α-OE + inhibitor group. The mean ± SEM was shown for all bar plots; $n = 5$.

demonstrate that either hypoxic exposure or exogenous overexpression of HIF-1α in PDAC cells promotes EMT and enhances cellular migratory and invasive capabilities, though the specific molecular mechanisms governing this process still require investigation.

DCLK1, a microtubule-associated protein originally identified in the nervous system, is thought to be involved in the microtubule regulation[29]. Recently, the role of DCLK1 beyond the nervous system has also been investigated, especially in tumor initiation, recurrence, and metastasis[30,31]. Bailey's team proposed DCLK1 as a cancer stem cell marker for PDAC in 2014, which labels a morphologically and functionally unique subset of stem-like cancer-initiating cells in preinvasive pancreatic lesions[19]. However, the potential interaction between hypoxic and DCLK1 in PDAC has not been elucidated.

Our bioinformatics data analysis results show that both HIF-1α and DCLK1 are upregulated in pancreatic tumors. The correlation coefficient between the two can reach 0.4, indicating a moderate positive correlation. Although there are some genes in the HIF pathway that have weak correlation with DCLK1, we speculate this may be due to the extremely high tumor heterogeneity within PDAC clinical samples. Such complex confounding factors inevitably reduce the linear correlation between individual hypoxia-related genes. Since HIF-1α is the most critical regulatory factor in the hypoxia process, we mainly focused on the correlation between HIF-1α and DCLK1 in this study.

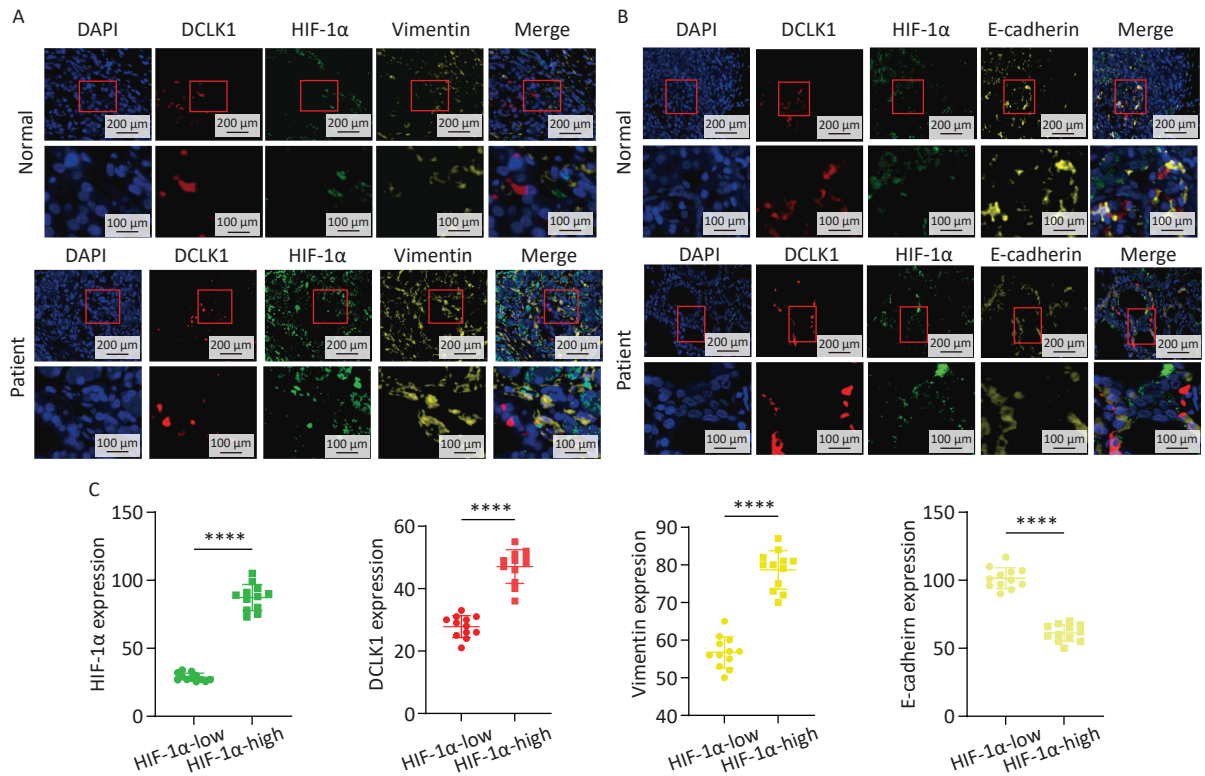

Figure 6. Clinical-spatial association of DCLK1, HIF-1α, and EMT markers in patients with PDAC. A, B. Representative images of multiplexed immunofluorescence analysis showed increased doublecortin-like kinase 1 (DCLK1), hypoxia-inducible factor-1α (HIF-1α), and Vimentin expression levels as well as decreased E-cadherin expression levels in pancreatic tumor tissues compared to pericancerous tissues. C. Quantitative analysis results showed DCLK1 and Vimentin expression levels are higher in the HIF-1α-high group, whereas the E-cadherin expression level was lower in the HIF-1α-high group than in the HIF-1α-low group. PDAC tissue microarray (TMA) samples were examined under a microscope at 20 × and 40 × magnification. Statistical significance was determined using the Student's *t*-test. Comparisons of differences between groups were indicated by $*P < 0.05$, $**P < 0.01$, $***P < 0.001$, and $****P < 0.0001$. The mean ± SEM is shown for all bar plots. HIF-1α-high group n=12, HIF-1α-low group n = 12.

To further verify the results of data analysis, we conducted a series of *in vitro* experiments and confirmed that when HIF-1α is overexpressed, the expression level of DCLK1 subsequently increases. When cells are cultured under hypoxic conditions and treated with a HIF-1α inhibitor or HIF-1α knockdown, a marked reduction in DCLK1 expression is observed. These findings indicate a positive correlation between HIF-1α and DCLK1, and suggest that DCLK1 is expressed downstream of HIF-1α. Furthermore, ChIP-qPCR experiments confirmed that HIF-1α directly binds to the HRE motif in the regulatory region of DCLK1, providing direct molecular evidence for the conclusion that DCLK1 is transcriptionally upregulated by HIF-1α in pancreatic cancer cells. This regulatory axis has not been clearly defined in previous studies.

Subsequently, our study revealed that DCLK1 promotes pancreatic cancer malignancy in hypoxic microenvironments. Both subcutaneous xenograft growth and tail vein injection metastasis model further confirmed that DCLK1 contributes to tumor growth and metastatic progression *in vivo*. However, there are still certain limitations in our animal models: we mainly used HIF-1α-overexpressing cells instead of establishing genuine hypoxic conditions, which may not fully recapitulate the authentic hypoxic microenvironment. In future studies, we will validate our current findings under physiological hypoxic conditions to further confirm our research conclusions.

In addition to *in vitro* and *in vivo* experiments, we also observed the correlation between HIF-1α and the survival prognosis of PDAC patients in human tissue samples. Using large public mRNA cohorts (the 178-patient TCGA cohort and GEO database), we demonstrated that patients with high hypoxia scores or high HIF-1α mRNA expression have poorer survival outcomes. Furthermore, IHC results preliminarily confirmed the association between HIF-1α protein level and pathological grade. Nevertheless, our study is limited by the small sample size of our in-house IHC cohort (n = 15), which prevented us from performing multivariate survival analysis. Further validation in a larger, multi-center PDAC cohort is required in future studies.

In summary, this study explored that in PDAC, a highly malignant tumor, the hypoxic microenvironment can upregulate the expression of HIF-1α, which in turn promotes the expression of DCLK1 and facilitates the malignant biological behavior of tumor cells. Therefore, targeting DCLK1 is a promising therapeutic strategy for pancreatic cancer with hypoxic characteristics.

Funding This work was supported by the Beijing Natural Science Foundation (No. 7232064).

Authors' Contributions Conceptualization and study design: Yang Ge and Hua Fan; Data acquisition: Rui Yan and Yunting Bai; Data analysis: Rui Yan; Manuscript drafting: Rui Yan and Yunting Bai; Experimental data contribution: Patiguli Yisilamu; Manuscript revision: Yang Ge, Guangyu; Statistical analysis: Ziwei Liang. All the authors have read and approved the final version of the manuscript.

Competing Interests The authors declare that they have no conflict of interest.

Ethics This study was approved by the Clinical Research Ethics Committee of the Beijing Chao-Yang Hospital, Capital Medical University, Beijing, China. Informed consent was obtained from each patient. The animal study protocol was approved by the Animal Ethics Committee of the Capital Medical University (approval no. 25-2157).

Acknowledgements We express our sincere appreciation to all those who contributed to improving this manuscript.

Data Sharing The datasets generated for this study are available on request to the corresponding author. The supplementary materials will be available in www.besjournal.com.

Received: March 8, 2026;
Accepted: June 11, 2026

REFERENCES

1. Chen WQ, Zheng RS, Baade PD, et al. Cancer statistics in China, 2015. CA Cancer J Clin, 2016; 66, 115−32.
2. Siegel RL, Miller KD, Wagle NS, et al. Cancer statistics, 2023. CA Cancer J Clin, 2023; 73, 17−48.
3. Chen XC, Zhong FF, Li J. Trends of disease burden of pancreatic cancer attributed to high fasting plasma glucose in China, 1990-2021: insights from the global burden of disease study 2021. Biomed Environ Sci, 2025; 38, 379−84.
4. Tao JX, Yang G, Zhou WC, et al. Targeting hypoxic tumor microenvironment in pancreatic cancer. J Hematol Oncol, 2021; 14, 14.
5. Infantino V, Santarsiero A, Convertini P, et al. Cancer cell metabolism in hypoxia: role of hif-1 as key regulator and therapeutic target. Int J Mol Sci, 2021; 22, 5703.
6. Lin JW, Wang XJ, Zhai SY, et al. Hypoxia-induced exosomal circPDK1 promotes pancreatic cancer glycolysis via c-myc activation by modulating miR-628-3p/BPTF axis and degrading BIN1. J Hematol Oncol, 2022; 15, 128.
7. Wicks EE, Semenza GL. Hypoxia-inducible factors: cancer progression and clinical translation. J Clin Invest, 2022; 132, e159839.
8. Majmundar AJ, Wong WJ, Simon MC. Hypoxia-inducible factors and the response to hypoxic stress. Mol Cell, 2010; 40,

294−309.
9. Yfantis A, Mylonis I, Chachami G, et al. Transcriptional response to hypoxia: the role of HIF-1-associated co-regulators. Cells, 2023; 12, 798.
10. Wenger RH, Stiehl DP, Camenisch G. Integration of oxygen signaling at the consensus HRE. Sci STKE, 2005; 2005, re12.
11. Galbán S, Gorospe M. Factors interacting with HIF-1α mRNA: novel therapeutic targets. Curr Pharm Des, 2009; 15, 3853−60.
12. Bao B, Ali S, Ahmad A, et al. Differentially expressed miRNAs in cancer-stem-like cells: markers for tumor cell aggressiveness of pancreatic cancer. Stem Cells Dev, 2014; 23, 1947−58.
13. Zhao Y, Xing C, Deng YT, et al. HIF-1α signaling: essential roles in tumorigenesis and implications in targeted therapies. Genes Dis, 2024; 11, 234−51.
14. Nevi L, Di Matteo S, Carpino G, et al. DCLK1, a putative stem cell marker in human cholangiocarcinoma. Hepatology, 2021; 73, 144−59.
15. Yao JN, Huang XY, Sun QQ, et al. Hypoxic stimulation of DCLK1 transcription and alternative-promoter switching fuels tumor malignancy in clear cell renal cell carcinoma. Cell Death Dis, 2025; 16, 594.
16. Ali N, Nguyen CB, Chandrakesan P, et al. Doublecortin-like kinase 1 promotes hepatocyte clonogenicity and oncogenic programming via non-canonical β-catenin-dependent mechanism. Sci Rep, 2020; 10, 10578.
17. Sureban SM, May R, Lightfoot SA, et al. DCAMKL-1 regulates epithelial-mesenchymal transition in human pancreatic cells through a *miR-200a*-dependent mechanism. Cancer Res, 2011; 71, 2328−38.
18. Sureban SM, May R, Mondalek FG, et al. Nanoparticle-based delivery of siDCAMKL-1 increases *microRNA-144* and inhibits colorectal cancer tumor growth via a Notch-1 dependent mechanism. J Nanobiotechnol, 2011; 9, 40.
19. Bailey JM, Alsina J, Rasheed ZA, et al. DCLK1 marks a morphologically distinct subpopulation of cells with stem cell properties in preinvasive pancreatic cancer. Gastroenterology, 2014; 146, 245−56.
20. Westphalen CB, Takemoto Y, Tanaka T, et al. Dclk1 defines quiescent pancreatic progenitors that promote injury-induced regeneration and tumorigenesis. Cell Stem Cell, 2016; 18, 441−55.
21. Di Giovannantonio M, Hartley F, Elshenawy B, et al. Defining hypoxia in cancer: a landmark evaluation of hypoxia gene expression signatures. Cell Genomics, 2025; 5, 100764.
22. Moore LL, Houchen CW. Evolving insights into pancreatic tumor initiation and progression through DCLK1-expressing tuft cells. Dev Cell, 2025; 60, 817−8.
23. Ding L, Yang YN, Ge Y, et al. Inhibition of DCLK1 with DCLK1-IN-1 suppresses renal cell carcinoma invasion and stemness and promotes cytotoxic T-cell-mediated anti-tumor immunity. Cancers, 2021; 13, 5729.
24. Ferguson FM, Nabet B, Raghavan S, et al. Discovery of a selective inhibitor of doublecortin like kinase 1. Nat Chem Biol, 2020; 16, 635−43.
25. Cai J, Chen HD, Lu M, et al. Advances in the epidemiology of pancreatic cancer: trends, risk factors, screening, and prognosis. Cancer Lett, 2021; 520, 1−11.
26. Huang JJ, Lok V, Ngai CH, et al. Worldwide burden of, risk factors for, and trends in pancreatic cancer. Gastroenterology, 2021; 160, 744−54.
27. Keith B, Johnson RS, Simon MC. HIF1α and HIF2α: sibling rivalry in hypoxic tumour growth and progression. Nat Rev Cancer, 2012; 12, 9−22.
28. Semenza GL. Hypoxia-inducible factors in physiology and medicine. Cell, 2012; 148, 399−408.
29. Westphalen CB, Quante M, Wang TC. Functional implication of Dclk1 and Dclk1-expressing cells in cancer. Small GTPases, 2017; 8, 164−71.
30. Cao ZY, Weygant N, Chandrakesan P, et al. Tuft and cancer stem cell marker DCLK1: a new target to enhance anti-tumor immunity in the tumor microenvironment. Cancers, 2020; 12, 3801.
31. Velázquez-Enríquez JM, Cerna R, Beltrán-Ramírez O, et al. DCLK1 is overexpressed and associated with immune cell infiltration in hepatocellular carcinoma. Biochem Genet, 2024; 62, 4280−302.